Cerebral Cortex Advance Access published May 8, 2014

Cerebral Cortex
doi:10.1093/cercor/bhu084

Asymmetry of White Matter Pathways in Developing Human Brains

Jae W. Song[1,2,7], Paul D. Mitchell[4], James Kolasinski[5,8], P. Ellen Grant[1,2,3,5], Albert M. Galaburda[6] and Emi Takahashi[1,2,5]

[1]Department of Medicine, Division of Newborn Medicine, [2]Fetal-Neonatal Neuroimaging and Developmental Science Center and, [3]Department of Radiology, Boston Children's Hospital, Harvard Medical School, Boston, MA 02115, USA, [4]Clinical Research Center, Boston Children's Hospital, Boston, MA 02115, USA, [5]Athinoula A. Martinos Center for Biomedical Imaging, Massachusetts General Hospital, Harvard Medical School, Charlestown, MA 02129, USA, [6]Department of Neurology, Division of Cognitive Neurology, Beth Israel Deaconess Medical Center, Harvard Medical School, Boston, MA 02115, USA, [7]Current address: Department of Radiology, Yale University School of Medicine, New Haven, CT 06510, USA and [8]Current address: Centre for Functional Magnetic Resonance Imaging of the Brain (FMRIB), Nuffield Department of Clinical Neurosciences, University of Oxford, Oxford OX3 9DU, UK

Address correspondence to Dr Emi Takahashi, Division of Newborn Medicine, Department of Medicine, Boston Children's Hospital, Harvard Medical School, Boston, MA, USA. Email: emi@nmr.mgh.harvard.edu

Little is known about the emergence of structural asymmetry of white matter tracts during early brain development. We examined whether and when asymmetry in diffusion parameters of limbic and association white matter pathways emerged in humans in 23 brains ranging from 15 gestational weeks (GW) up to 3 years of age (11 ex vivo and 12 in vivo cases) using high-angular resolution diffusion imaging tractography. Age-related development of laterality was not observed in a limbic connectional pathway (cingulum bundle or fornix). Among the studied cortico-cortical association pathways (inferior longitudinal fasciculus [ILF], inferior fronto-occipital fasciculus, and arcuate fasciculus), only the ILF showed development of age-related laterality emerging as early as the second trimester. Comparisons of ages older and younger than 40 GW revealed a leftward asymmetry in the cingulum bundle volume and a rightward asymmetry in apparent diffusion coefficient and leftward asymmetry in fractional anisotropy in the ILF in ages older than 40 GW. These results suggest that morphometric asymmetry in cortical areas precedes the emergence of white matter pathway asymmetry. Future correlative studies will investigate whether such asymmetry is anatomically/genetically driven or associated with functional stimulation.

Keywords: asymmetry, brain, development, diffusion imaging, human, tractography, white matter

Introduction

The 2 hemispheres of the human brain contribute asymmetrically to information processing. One of the most strikingly lateralized functions in the human is language, several aspects of which are predominantly processed in the left hemisphere in adults. In addition to recent studies suggesting that left–right differentiation of structure and function enhances the functional capacity of the brain (e.g., Halpern et al. 2005), clinically, developmental dyslexia (Galaburda et al. 1985; Galaburda 1993; Jenner et al. 1999), schizophrenia (Ribolsi et al. 2009; Oertel-Knochel and Linden 2011), and autism (Escalante-Mead et al. 2003; Herbert et al. 2005) are often linked to abnormal brain lateralization.

Asymmetries of brain surface morphometry emerge as early as the fetal stage (Hochestetter 1929; Fontes 1944; Chi et al. 1977; Heilbroner and Holloway 1988; Gilmore et al. 2007; Hill et al. 2010; Kasprian et al. 2011). Although a few groups have reported the overall development of white matter at fetal ages by using diffusion tractography (e.g., Kostovic and Vasung, 2009; Vasung et al. 2010; Takahashi et al. 2012), asymmetry in specific white matter tract pathways has only been reported in older ages, such as in children and adults (Lebel and Beaulieu 2009; Thiebaut de Schotten et al. 2011). For example, in children (>5 years old) and adults, the right inferior fronto-occipital fasciculus (IFOF), the left inferior longitudinal fasciculus (ILF) (Thiebaut de Schotten et al. 2011) and left arcuate fasciculus (AF) (Lebel and Beaulieu 2009) reveal early lateralized development, suggesting that asymmetry probably emerges in association pathways earlier than 5 years of age. In fact, significant neuroanatomic changes occur even earlier and during the first year of life (Provenzale et al. 2007). However, asymmetry of brain pathways in early development, as disclosed by imaging techniques, has not yet been directly addressed, because of several challenges related to MR imaging (e.g., motion in living fetuses in utero, the small size of the fetal brain, and less myelination, which requires very high spatial resolution for revealing detailed pathways) as well as the availability of fetal brains.

High-angular resolution diffusion imaging (HARDI) tractography enables identification of complex crossing tissue coherence in the brain (Tuch et al. 2003) even in immature brains (Takahashi et al. 2011, 2012), which are typically more challenging to segment due to a surplus of unmyelinated fibers. In this study, HARDI tractography was used to identify several white matter pathways, including limbic (cingulum bundle and fornix) and association (ILF, IFOF, and AF) pathways. Volume and diffusion properties [fractional anisotropy (FA) and apparent diffusion coefficient (ADC)] were obtained on the identified tracts to explore their emerging asymmetry. The aim of this study was to identify the temporal emergence of white matter pathways as detected by diffusion tractography and describe a spatio-temporal asymmetry between hemispheres in developing human brains starting as early as the second trimester. We hypothesized that, by term, asymmetry in white matter pathways thought to be linked to primary associative functions would be present earlier than pathways associated with higher cognitive functions.

Methods

Fetal Brain Specimens

Twenty-three brains were imaged for this study. Table 1 reports the age brackets, the number of specimens, and whether the brain was imaged ex vivo or in vivo. The ages were expressed as postgestational weeks (GW), which equal gestational age plus postnatal age. Seven postmortem brains were obtained from the Department of Pathology,

Table 1
Characteristics of brains

Subject	Source	Age	Brain image
1	BWH	15 GW	Ex vivo
2	BWH	17 GW	Ex vivo
3	AIBB	19 GW	Ex vivo
4	BWH	20 GW	Ex vivo
5	BWH	20 GW	Ex vivo
6	BWH	20 GW	Ex vivo
7	BWH	21 GW	Ex vivo
8	BWH	21 GW	Ex vivo
9	AIBB	21 GW	Ex vivo
10	AIBB	22 GW	Ex vivo
11	BCH	30 GW	In vivo
12	BCH	30 GW	In vivo
13	BCH	34 GW	In vivo
14	BCH	40 GW	In vivo
15	BCH	40 GW	In vivo
16	BCH	40 GW	In vivo
17	BCH	40 GW	In vivo
18	AIBB	8 months[a]	Ex vivo
19	BCH	20 months [a]	In vivo
20	BCH	2 years[a]	In vivo
21	BCH	3 years[a]	In vivo
22	BCH	3 years[a]	In vivo
23	BCH	3 years[a]	In vivo

GW, gestational week; BWH, Brigham and Women's Hospital; AIBB, Allen Institute Brain Bank; BCH, Boston Children's Hospital.
[a]For analyses, all ages were scaled to weeks by adding 40 weeks. For instance, 8 months as 72 weeks, 20 months as 120 weeks, 2 years as 144 weeks, and 3 years as 196 weeks.

Brigham and Women's Hospital (BWH; Boston, MA, USA), and 4 postmortem brains (19, 21, and 22 GW, and 8M) were provided by the Allen Institute Brain Bank (AIBB; Seattle, WA, USA). Postmortem specimens were obtained with full parental consent. The primary cause of death was complications of prematurity. The brains were grossly normal, and standard autopsy examinations of all brains undergoing postmortem HARDI revealed minimal or no pathologic abnormalities at the macroscopic level. Ex vivo fetal and postnatal brains and living postnatal infant brains were included in the study, which allowed us to reveal brain structure in unforeseen detail. Although ex vivo imaging is superior, we have previously shown that ex vivo and in vivo imaging produce comparable tracking results at fetal, neonatal, and toddler ages (Xu et al. 2014).

All living participants (12 newborns and children) had clinically indicated brain MRI studies that were diagnostically interpreted to show no abnormalities. Indications for imaging included concern for hypoxic ischemic injury, apnea, and transient choreiform movements after an upper respiratory tract infection. None had clinical concerns for a congenital malformation or genetic disorder. All research protocols were approved by the institutional review board.

Tissue Preparation for HARDI

At the time of autopsy, all brains were immersion fixed. The brains from BWH were stored in 4% paraformaldehyde, and the brains from AIBB were stored in 4% periodate-lysine-paraformaldehyde (PLP). During MR image acquisition, BWH brains were placed in Fomblin solution (Ausimont, Thorofare, NJ, USA) (e.g., Takahashi et al. 2012) and AIBB brains were placed in 4% PLP. While these different solutions tend to change the background contrast (i.e., we see a dark background outside of the brain using Fomblin, and a bright background using PLP), these solutions do not specifically change diffusion properties (e.g., FA and ADC) within the brain parenchyma.

Diffusion MRI Procedures

Different scanner systems were used to accommodate different brain sizes. Magnetic resonance (MR) coils that best fit each brain sample were used to ensure optimal imaging. The postmortem brain specimens from BWH were imaged with a 4.7 T Bruker Biospec MR system (specimens from 15 to 21 GW), and specimens from the AIBB were imaged with a 3 T Siemens MR system (3 fetal [19, 21, 22 GW] and 8M specimens) at the A. A. Martinos Center, Massachusetts General Hospital, Boston, MA, USA. The 3 T system was used to accommodate the AIBB brains that were in cranio and did not fit in the 4.7 T bore. To improve the imaging quality and obtain the best signal-to-noise ratio and high spatial resolution, we used custom-made MR coils with one channel on the 4.7 and 3 T systems (Takahashi et al. 2012; Kolasinski et al. 2013; Xu et al. 2014).

For the BWH brains, a 3D diffusion-weighted spin-echo echo-planar imaging (SE-EPI) sequence was used with a repetition time/echo time (TR/TE) of 1000/40 ms, with an imaging matrix of $112 \times 112 \times 112$ pixels. Sixty diffusion-weighted measurements (with the strength of the diffusion weighting, $b = 8000$ s/mm^2) and one nondiffusion-weighted measurement (no diffusion weighting or $b = 0$ s/mm^2) were acquired with $\delta = 12.0$ ms and $\Delta = 24.2$ ms. The spatial resolution was $440 \times 500 \times 500$ μm. For the brains from the AIBB, diffusion-weighted data were acquired over 2 averages using a steady-state free-precession sequence with TR/TE = 24.82/18.76 ms, $\alpha = 60°$, and the spatial resolution was $400 \times 400 \times 400$ μm for brains at 19, 21, and 22 GW and $900 \times 900 \times 900$ μm for the 8M brain. Diffusion weighting was isotropically distributed along 44 directions ($b = 730$ s/mm^2) with 4 $b = 0$ images. We determined the highest spatial resolution for each brain specimen with an acceptable signal-to-noise ratio of more than 130.

The brains of living patients were imaged on a 3 T Siemens MR system, Boston Children's Hospital, Boston, MA, USA. The diffusion pulse sequence used for imaging live participants was a diffusion-weighted SE-EPI sequence, TR/TE 8320/88 ms, with an imaging matrix of $128 \times 128 \times 64$ pixels. The spatial resolution was $2 \times 2 \times 2$ mm. Thirty diffusion-weighted measurements ($b = 1000$ s/mm^2) and 5 nondiffusion-weighted measurements ($b = 0$ s/mm^2) were acquired with $\delta = 40$ ms and $\Delta = 68$ ms.

Reconstruction and Identification of Tractography Pathways

White matter tracts were reconstructed in each brain with the Diffusion Toolkit and TrackVis programs (http://trackvis.org). A streamline algorithm for diffusion tractography was used (Mori et al. 1999), as in previous publications (Schmahmann et al. 2007; D'Arceuil et al. 2008; Takahashi et al. 2010, 2011, 2012). The term "streamline" refers to connecting tractography pathways using a local maximum or maxima. This method is true for both DTI and HARDI. The streamline technique is limited in its ability to resolve crossing pathways when used with the traditional DTI technique, because one simply connects the direction of the principal eigen vector on a tensor to produce the DTI tractography pathways. This feature is a recognized limitation of DTI (Mori et al. 1999). Hence, in the current study, we used HARDI, which detects multiple local maxima on an orientation distribution function (ODF). Using each local maxima on an ODF, we applied the streamline algorithm to initiate and continue tractography (Tuch et al. 2003) using all the local maxima of an ODF to produce HARDI tractography pathways. This method enabled us to identify crossing pathways within a voxel.

Trajectories were propagated by consistently pursuing the orientation vector of least curvature. Tracking was terminated when the angle between two consecutive orientation vectors was greater than the given threshold (40°) or when the fibers extended outside of the brain surface. For the latter determination, mask (boundary) images of the brains created by MRIcro (www.sph.sc.edu/comd/rorden/mricro.html) were used in order to determine coherence in the brain itself and not in the surrounding immersion fluid. Of note, the mask image is a 3D binary image created from a mean diffusion image of each brain assessment with endpoints constrained to the brain tissue itself. The brain mask volumes were used to terminate tractography structures instead of the FA threshold (Schmahmann et al. 2007; Wedeen et al. 2008; Takahashi et al. 2010, 2012; Vishwas et al. 2010), because progressive myelination and crossing fibers in the developing brain can result in low FA values that may potentially incorrectly terminate tractography tracing in the gray matter.

The following 5 association pathways were segmented: the cingulum bundle, fornix, ILF, IFOF, and the arcuate fasciculus (AF). Briefly, following previously described methods (Catani and Thiebaut de Schotten 2008), a two-ROI approach was used to segment the ILF, inferior IFOF, AF, cingulum, and fornix. To identify tractography

pathways for the ILF, we placed an ROI in the occipital and anterior temporal regions and restricted tracking to pathways running only between these 2 ROIs. This method identifies the ILF from the uncinate as well as other pathways. For visualization purposes in Figure 1, the number of detected tractography connections were restricted by 75% of the connections that touched an axial slice (Fig. 1, left) and a sagittal

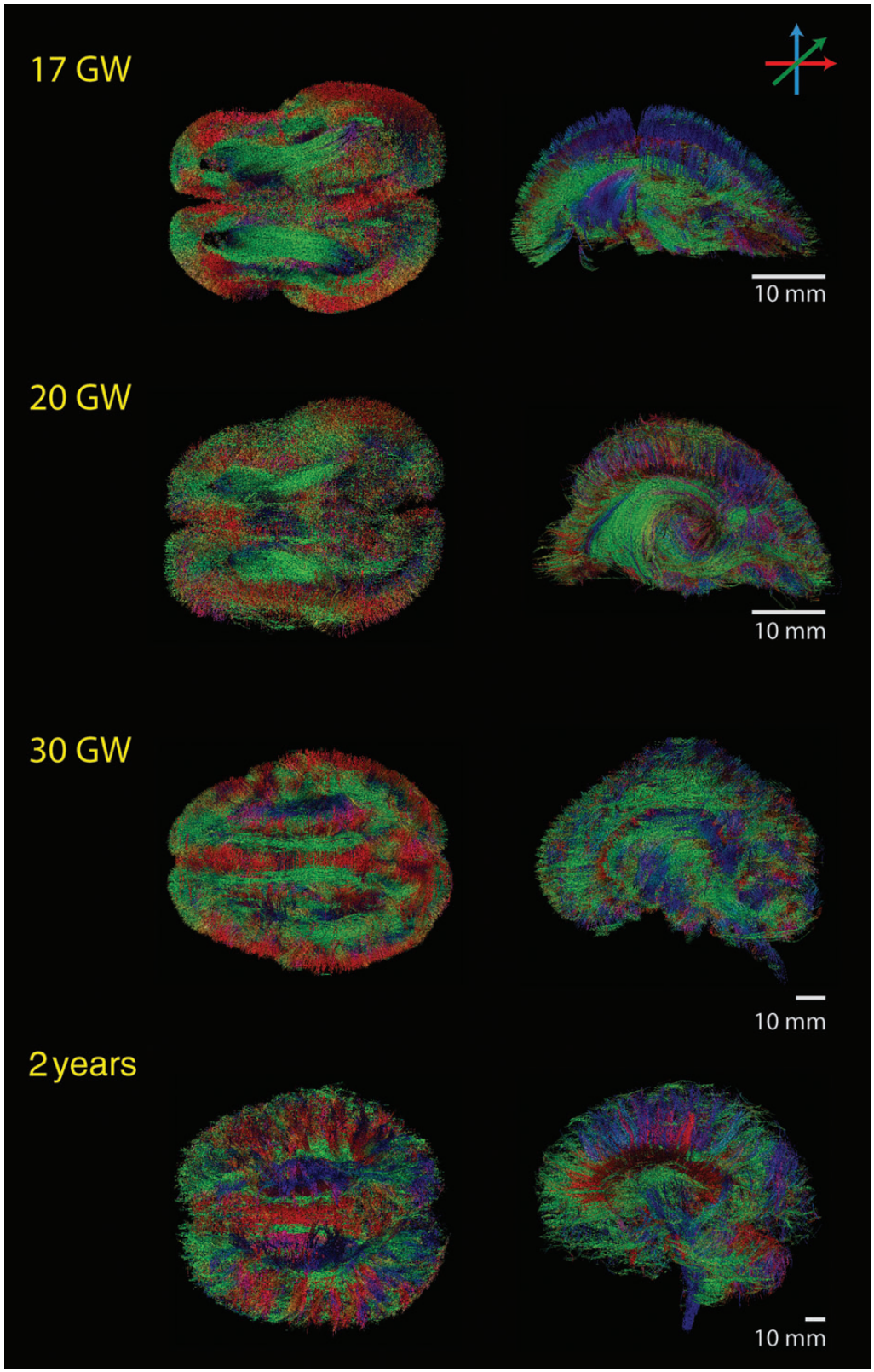

Figure 1. Maximum projection images of whole brains at different ages. Axial and sagittal images of whole brains at selective references ages (17 GW to 2 years) are shown. Note the differences in scale of the brains, indicating a rapid growth in both size and shape.

slice (Fig. 1, right) with a thickness of 10 voxels. Tractography pathways were then restricted to start and end within the plane. Of note, the emergence of white matter tracts will be written to mean the detection of fibers by diffusion tractography.

The color-coding of tractography pathways in Figures 1 and 2 was based on a standard red-green-blue code that was applied to the vector in each brain area to show the direction of the tractography pathways (green for right-left, red for dorsal-ventral, and blue for anterior-posterior, the latter in pathways that are confined to the coronal slice analyzed).

Statistical Analysis

The measures of FA, ADC, and volume are automatically derived by TrackVis for each segmented pathway after FA and ADC maps of the whole brain are loaded. FA, ADC, and volume outcomes of each segmented pathway were obtained. The volume of pathways was calculated by counting the number of voxels that touched or passed through by the pathways.

The laterality index (LI) for FA (FA_{LI}), ADC (ADC_{LI}), and volume (Vol_{LI}) of each white matter tract was compared at different developmental time points. LIs were calculated as follows: $LI = (L - R)/\{0.5 \times (L + R)\}$. LIs range from −2 to 2, and positive and negative LI values correspond to left- and rightward asymmetry, respectively (Galaburda et al. 1985; Caviness et al. 1996; Thiebaut de Schotten et al. 2011).

All statistical analyses were performed with SPSS version 19.0 (IBM SPSS, Chicago, IL, USA). To identify trends at each developmental time point, scatterplots were created for the continuous variables. Postmortem fixation processes may affect FA and ADC values and confound results. To account for such confounders, partial correlations with in vivo and ex vivo as the control variable were performed to facilitate comparisons across in vivo and ex vivo imaged brains. Additionally, subgroup correlation analyses of in vivo and ex vivo imaged brains were performed with Spearman's rank correlation. Box–whisker plots were generated to visualize the distributions, and the Mann–Whitney *U*-test was performed to compare the LIs by age. Statistical significance was set at $P < 0.05$.

Results

Qualitative Description of the Development of White Matter Pathways

The fornix was thickest at 21 GW and gradually thinned with age. The cingulum bundle was smooth and thin until 21 GW

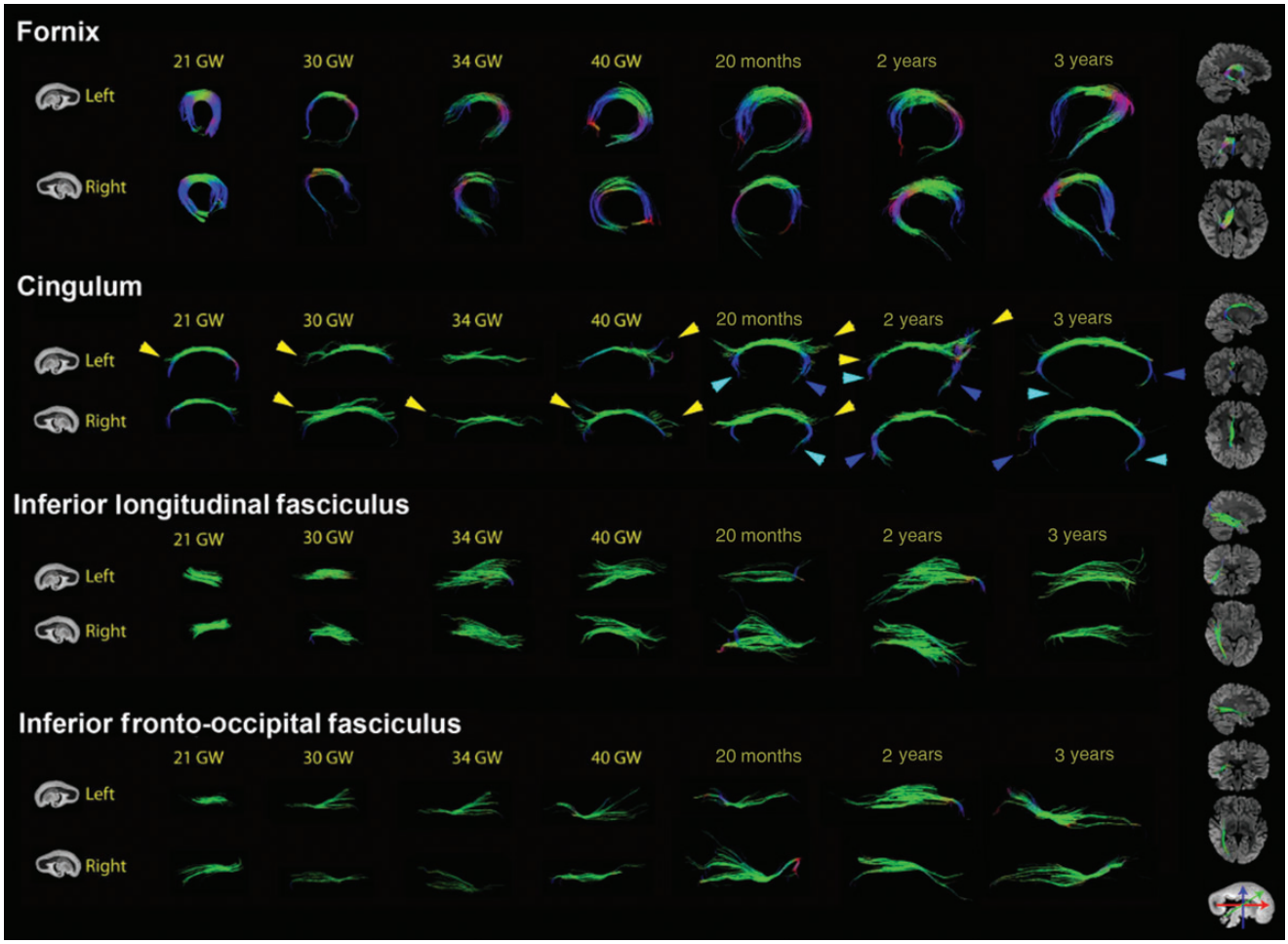

Figure 2. Development of white matter tract pathways. Tractography at several reference ages of the fornix, cingulum bundle, ILF, and IFOF are shown for the left and right hemispheres. As a reference, the right-most column illustrates the white matter tract against brain background images in sagittal, coronal, and axial slices. The left-most column illustrates a reference brain for orientation. Between 21 and 30 GW, the caliber of the fornix markedly diminished in thickness. The left cingulum bundle extended tractography fibers anteriorly earlier on the left than on the right (yellow arrowheads; 21 GW). However, by 30 GW, anterior and posterior tractography fibers were seen arising from both the left and right cingulum bundles. At 40 GW, the right cingulum bundle showed increased branching fibers both anteriorly and posteriorly compared with the left. By 20 months, fibers extending to the infero-medial frontal regions (light blue arrowheads; 20 months, 2 years, 3 years) and parahippocampal regions were observed (dark blue arrowheads; 20 months, 2 years, 3 years). Both the ILF and IFOF became longer during development. Both pathways showed a fanned appearance posteriorly during similar ages of development (right ILF and IFOF, 34 GW; left ILF and IFOF, 20 months), which changed to a more elongated appearance by 3 years (see text for further details).

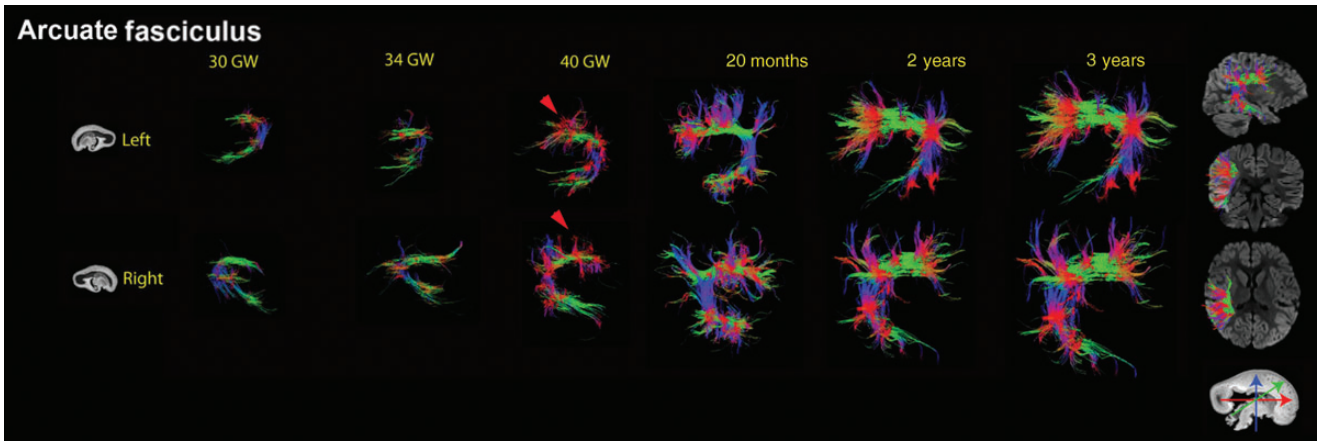

Figure 3. Development of the arcuate fasciculus. Tractography at several reference ages for the arcuate fasciculus (AF) are shown for each hemisphere. As a reference, the right-most column illustrates the white matter tract against a brain background image in sagittal, coronal, and axial slices. The left-most column illustrates a reference brain for orientation. The AF became evident by tractography by 30 GW. At 40 GW, short branching pathways from the main body of the tract were identified (red arrowheads), which gradually became longer at later developmental ages (see text for further details).

Table 2
Correlations of laterality indices by age[a]

Structure	Laterality index		
	LI_{Volume} versus age	LI_{FA} versus age	LI_{ADC} versus age
Cingulum bundle			
All data ($n = 19$)	0.44	0.02	0.02
In vivo ($n = 11$)	0.38	0.01	−0.06
Ex vivo ($n = 8$)	0.70	0.30	−0.05
Fornix			
All data ($n = 20$)	0.01	0.03	−0.01
In vivo ($n = 12$)	0.22	−0.03	−0.35
Ex vivo ($n = 8$)	−0.22	0.00	−0.18
Inferior longitudinal fasciculus			
All data ($n = 18$)	−0.13	0.53*	−0.46
In vivo ($n = 12$)	−0.28	0.63*	−0.61*
Ex vivo ($n = 7$)	0.93*	0.13	−0.10
Inferior fronto-occipital fasciculus[b]			
All data ($n = 15$)	0.02	−0.05	−0.01
In vivo ($n = 12$)	0.29	−0.16	−0.21
Arcuate fasciculus[c]			
In vivo ($n = 12$)	−0.24	0.32	−0.10

[a]Partial correlations with in vivo and ex vivo as a controlled variable were used for analyses including structures from both in vivo and ex vivo brains. Spearman correlations were used for subgroup analyses (in vivo and ex vivo separately).
[b]Inferior fronto-occipital fasciculi were present in $n = 3$ ex vivo brains.
[c]Arcuate fasciculus structures were segmented from in vivo scanned brains; none of the available ex vivo brain specimens revealed identifiable arcuate fasciculi.
*$P \leq 0.05$.

and revealed very short branches at both the anterior and posterior ends (Fig. 2, yellow arrowheads at 15 GW). The branching ends extended longitudinally with age and became more conspicuous at later ages (yellow arrowheads). The main body of the cingulum bundle did not extend into the ventral brain regions before 40 GW, but components of the bundle were observed extending to the medial, inferior frontal, and parahippocampal regions at 40 GW and later (Fig. 2, blue arrowheads).

The ILF was dense at 21 and 30 GW. Both the ILF and IFOF grew in length during development. The AF became evident by tractography by 30 GW. Until 34 GW, the AF was sparse, short and did not have obvious branches. At 40 GW, however, short branches arose from the main body of the tract (Fig. 3, red arrowheads; arrowheads are not shown in later ages to allow better visualization), and they became longer with age. The main body of the AF grew increasingly thicker by 3 years.

Overall, the thickness, density, and branching patterns of each pathway revealed subtle differences between the left and right sides.

Correlations Between Laterality Indices and Age

Correlations between age and laterality indices (LIs) for FA, ADC, and volume for each white matter tract are reported in Table 2 (see also associated scatterplots shown in Fig. 4). The LIs for each outcome weakly correlated with age in the cingulum bundle, fornix, IFOF, and AF ($r < 0.30$; Table 2). The cingulum bundle showed a marginally significant age-related leftward asymmetry in volume ($r = 0.44$, $P = 0.07$). Also, a significant age-related leftward asymmetry in FA for the ILF was seen during this period of development ($r = 0.53$, $P = 0.03$).

Subgroup analyses with in vivo and ex vivo imaged brains were also performed. This analysis showed significant results for the ILF. The ILF in in vivo imaged brains ($n = 12$; 30 GW to 3 years) showed a significant age-related leftward asymmetry with FA ($r = 0.63$, $P = 0.029$). Conversely, there was a significant age-related rightward asymmetry with ADC in the ILF pathways in in vivo imaged brains ($r = -0.61$, $P = 0.034$). In ex vivo imaged brains, there was a significant age-related leftward asymmetry in the volume of the ILF pathways ($n = 8$; 20 GW to 22 GW; $r = 0.93$, $P = 0.001$).

Comparisons of Laterality Indices Before and After 40 GW

Gross visual inspection of the scatterplots for volume, FA, and ADC LIs by age suggested a clustering of data points after 40 GW (Fig. 4). To further investigate this pattern, subgroup analyses by age were performed with in vivo imaged brains (Fig. 5), because this subgroup included brains both younger and older than 40 GW. Additionally, by only using in vivo data, confounding effects due to MRI scan conditions and fixation artifacts are reduced. The AF was not included in this analysis, because the former disappeared by 40 GW and only in vivo data were available for the AF. The ILF pathways showed significant leftward asymmetry in FA ($P = 0.007$) and rightward

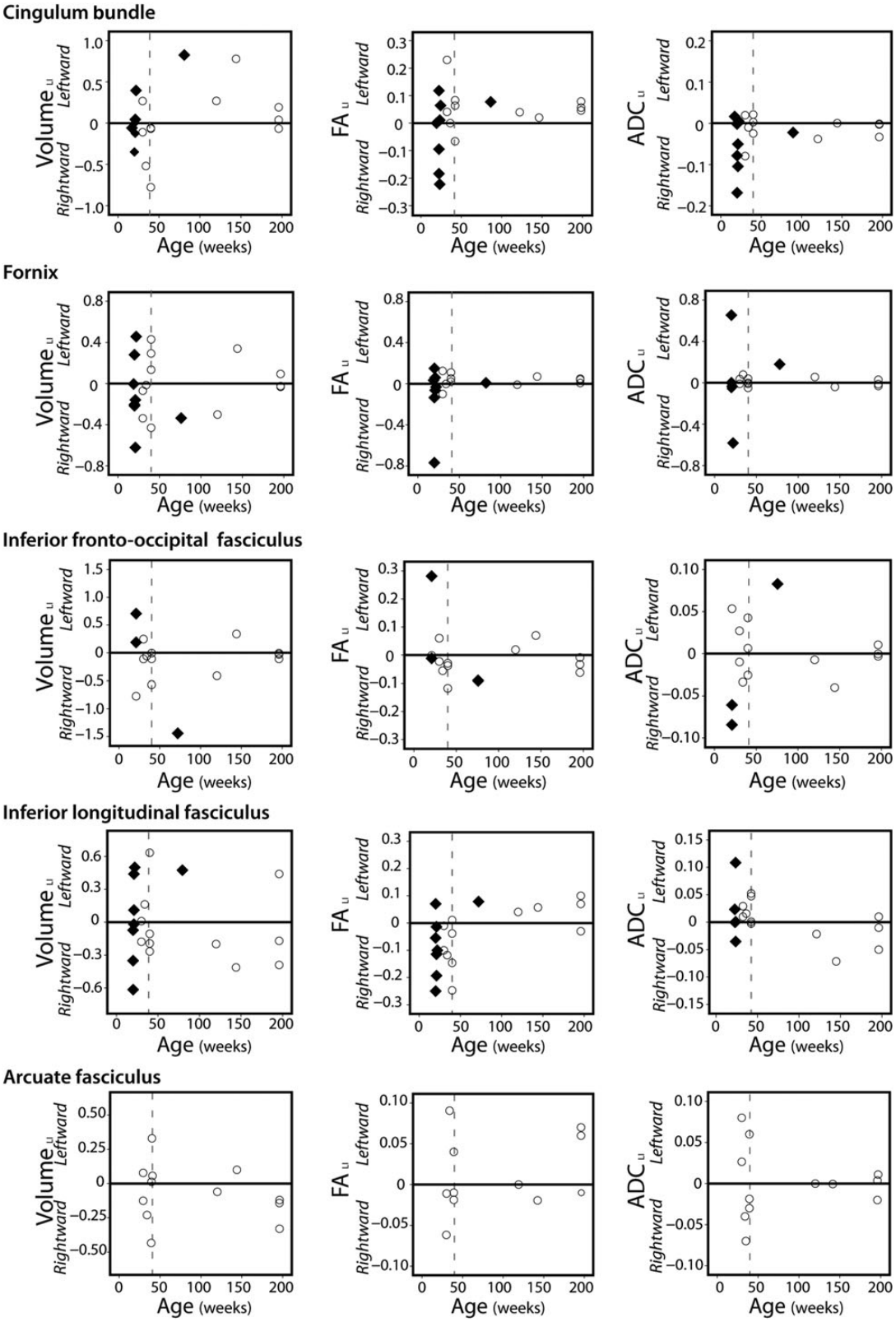

Figure 4. Scatterplots of laterality indices versus age. Scatterplots were generated for each white matter tract to visually examine age-related correlations between age (*x*-axis) versus the laterality index for FA, ADC, and volume (*y*-axis). A red dotted line was drawn at 40 GW. Datapoints comprising fetal ages <40 GW appeared scattered above and below the 0-line (horizontal black line; no asymmetry), likely representing interindividual variability. However, after 40 GW, most datapoints clustered above, below or at the 0-line. Open circles represent in vivo imaged brains, and solid diamonds represent ex vivo imaged brains.

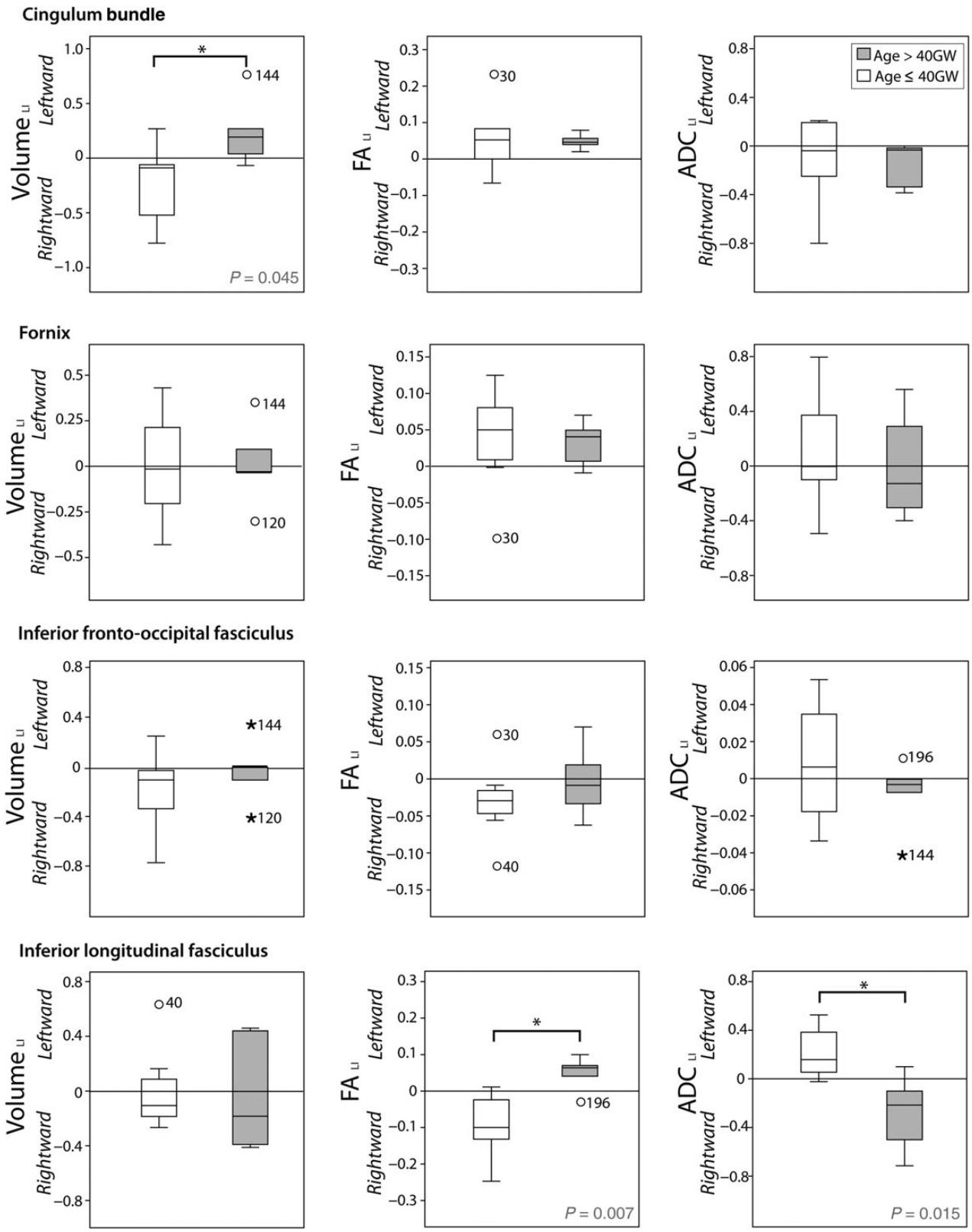

Figure 5. Comparison of laterality indices before and after 40 GW (using only in vivo data). Box–whisker plots were generated to compare the medians and distributions of the laterality index for each outcome by age. The cingulum bundle in brains aged >40 GW showed a significant leftward asymmetry in volume compared with brains aged <40 GW. The ILF showed a significant leftward asymmetry in FA and rightward asymmetry in ADC in brains aged >40 GW compared with brains aged <40 GW. The circles represent outliers and the asterisks represent extreme values at the respectively labeled ages in GW adjacent to the circle or asterisk {values greater than [2 × (1.5 × interquartile range)]}.

asymmetry in ADC ($P = 0.015$) in brains aged >40 GW when compared with brains aged ≤40 GW (Fig. 5). Additionally, the cingulum bundle showed significant leftward asymmetry in volume in brains aged >40 GW when compared with brains aged ≤40 GW ($P = 0.045$).

Discussion

Using diffusion tractography, we investigated the temporal emergence of white matter tracts and their developing asymmetry in human brains from 15 GW to 3 years. Significant age-related leftward hemispheric asymmetry in the ILF pathway in FA emerged as early as 15 GW. In contrast, asymmetry of the white matter pathways associated with higher order cognitive functions, such as the AF, was not observed up to 3 years of age. These results suggest that although emerging asymmetry of white matter pathways is prenatally present, more robust asymmetry likely emerges postnatally.

Limbic Pathways

Age-related correlations with FA_{LI}, ADC_{LI}, and Vol_{LI} were not observed in the fornix and cingulum bundle (Table 2). The result in the fornix is consistent with the literature (Thiebaut de Schotten et al. 2011). Interestingly, although several studies report leftward asymmetry in FA of adult cingulum bundles (Gong et al. 2005; Takao et al. 2011; Yin et al. 2013), we did not see a significant age-related correlation for the cingulum bundle. Developing regional asymmetry among the different segments of the cingulum bundle may explain why there was no significant asymmetry in FA. Gong et al. (2005) segmented the cingulum bundle in adult humans into multiple parts and reported leftward asymmetry in the anterior segments. Given the general posterior–anterior direction of white matter development, perhaps during the early developmental ages, posterior segments of the cingulum bundle mature earlier.

Association Pathways

We hypothesized that asymmetry in white matter pathways thought to be linked to primary associative functions would be present earlier than in pathways associated with higher cognitive functions. A previous research study proved that HARDI tractography can reliably resolve crossing white matter pathways along the ILF (Berman et al. 2013). Interestingly, although both the ILF and IFOF pathways are associated with visual processes (Chechlacz et al. 2012), our results showed asymmetry in the ILF but not the IFOF during the studied ages. The ILF, which extends from the occipital to the temporal lobes (Schmahmann and Pandya 2009), is thought to be associated with object recognition. Indeed, children with an object recognition deficit revealed a significantly decreased mean-FA of the ILF in the left hemisphere with resultant loss of asymmetry of the ILF pathway (Ortibus et al. 2012). Compatible with the results of Ortibus et al., our study revealed a significant age-related leftward asymmetry in FA of the ILF pathway.

In contrast, the IFOF revealed no significant age-related asymmetry, which suggests that asymmetry in tracts associated with object recognition likely precedes asymmetry in tracts involved in a more integrative role. In fact, the IFOF is a cortico-cortical pathway extending from the occipital to inferior frontal lobes and is thought to play an integrative role in visual processing, such as emotion recognition through facial expressions (Philippi et al. 2009). In the adult brain, laterality in both the ILF and IFOF has been described (Thiebaut de Schotten et al. 2011; Kucyi et al. 2012), indicating that asymmetry eventually develops. Studies suggest that cortical maturation is directional with the inferior temporal and inferior frontal lobes being the last regions to mature (Gogtay et al. 2004; Takahashi et al. 2012). Hence, given the ages studied, asymmetry in the IFOF, a ventral pathway, may emerge outside the ages analyzed in this study.

The results of the ILF and IFOF pathways raise an interesting developmental difference in white matter pathway and sulcal asymmetry. Robust sulcal asymmetry is described in the temporal lobes starting in the late second trimester (Rajagopalan et al. 2011). This contrasts with the degree of white matter pathway asymmetry in the same region at the same developmental stage. One explanation is that early brain growth may be driven primarily by gray matter rather than white matter. During the first year of life, gray matter accounting for hemispheric growth was reported to increase by 149% contrasting with an 11% increase in white matter volume (Knickmeyer et al. 2008). The changes seen in sulcation of the cortical gray matter may thus be driven by the dramatic changes in gray matter volume, whereas white matter tract asymmetry may be related to functional stimulation.

Arcuate Fasciculus

Despite many studies indicating a leftward laterality in the adult AF (Buchel et al. 2004; Takao et al. 2011), no asymmetry was observed in the AF up to 3 years of age. This finding may be explained by the developmental direction of white matter maturation. Thiebaut de Schotten and colleagues (2011) segmented the adult AF into posterior, anterior, and long segments and found asymmetry in the anterior and long segments but no asymmetry in the posterior segment. Thus, with the general posterior–anterior direction of white matter development, the posterior segment may mature earlier and have a dominating effect in overall volume, FA, and ADC laterality.

Furthermore, studies suggest asymmetry in AF connectivity develops contemporaneously with language and reading acquisition. Literacy is thought to reinforce left temporoparietal connections and the microstructure of the AF, as seen by one study comparing the AF of literates and illiterates (Dehaene et al. 2010; Thiebaut de Schotten et al. 2011). With reading acquisition, the functional activation of the planum temporale, an important source of axons to the AF, was seen to be dramatically asymmetric in favor of the left side (Dehaene-Lambertz et al. 2006). Furthermore, it is not until age 3–4 years that children begin to use sentences with more than 4 words to meet their language-related developmental milestones (Simms and Schum 2011). Hence, robust asymmetry in the AF probably emerges after 3 years of age.

Limitations of the Current Study

There are several limitations in this study. First, both ex vivo and in vivo data were combined in some of the analyses, which may result in variations of postmortem conditions, specifically in ex vivo MR imaging. However, ex vivo imaging, especially of fetal brains, provides high-resolution tractography, which enables greater understanding of fetal brain connectivity. Obtaining the same degree of resolution from in utero imaging remains challenging. Nevertheless, we acknowledge this

limitation and control for differences between the 2 groups by statistical methods, such as partial correlation analyses. We also perform subgroup analyses with only in vivo brains to draw conclusions about emerging laterality (Fig. 5).

Second, the number of brains at each age is few, and the study is limited by brains aged up to 3 years. Future studies will aim to have a larger sample size with brains at a wider age interval to further investigate the development of asymmetry in white matter tract pathways. With older ages, additional functional information can be collected. For instance, insight on the effects of language acquisition on structural white matter tract asymmetry during development could shed light on when is the most vulnerable periods during brain development. Additionally, hand dominance is also known to be strongly lateralized in the human brain. The literature regarding handedness and brain asymmetry remains conflicting. Whether hand dominance influences white matter tract asymmetry at these early developmental stages also remains unclear. Future studies will aim to take a systematic approach to investigating the development of asymmetry by age, while taking into account other factors, such as gender, language acquisition, and hand dominance.

Future Directions

Understanding fetal and neonatal brain connectivity is a challenging but common goal in developmental neurobiology. Challenges are related to the dynamic changes that occur throughout development as well as the presence of exuberant axons at these early ages. Many lines of evidence show that the developing neural network is first established by a surplus of connections that subsequently undergo a refinement process of developmental axon pruning (Huttenlocher 1979; Innocenti et al. 1986; LaMantia and Rakic 1990; Huttenlocher and Dabholkar 1997). Compatible with the literature, our results also show that white matter pathways involved in higher-order cognitive or integrative functions, such as the AF and IFOF, are initially symmetric. Developmental axon pruning mechanisms likely follow and refine axonal connections mediating the development of asymmetry. Glial lysosomal activity has previously been shown to be a central feature of developmental axon pruning (Song et al. 2008), and in the future, contrast agents with the ability to mark increased areas of glial lysosomal activity may be a potential means for highlighting regions of developmental axon pruning that lead to structural asymmetry.

This study focused on the development of white matter tracts that exist completely in their respective hemispheres. Commissural fibers, such as the corpus callosum and the anterior and posterior commissures, were not included in this study as they are midline structures. The growth of the corpus callosum was observed from 4 GW (Rakic and Yakovlev 1968), and the maturation of the commissure pathways has been reported to be more prolonged than the association fibers with development continuing well into the mid-20s (Lebel et al. 2008). It has, however, been shown that similar developmental phenomena occur in the corpus callosum in rhesus monkeys, whereby exuberant axons are selectively eliminated, generating asymmetry if an unequal number of axons are pruned on each side (LaMantia and Rakic 1990). Hence, although for anatomic and temporal reasons, we felt including these fibers were out of the scope of this study, future studies will further investigate the asymmetry of these midline structures by tractography.

Whether functional asymmetry precedes structural refinement still remains unclear. Correlating functional MRI and tractography with probabilistic estimations (e.g., Takahashi et al. 2007, 2013; Berman et al. 2013) to elucidate a temporal relationship between structural and functional laterality is also a future aim. Moreover, the role of gender in white matter tract asymmetry will be examined with the recruitment of a larger sample size and wider range of ages. Establishing a functional and structural map for normal development of asymmetry will provide additional insight about cognitive development in children and identify the most vulnerable periods of white matter pathway development, which may affect children with learning disabilities.

Funding

This work was supported the Eunice Shriver Kennedy National Institute of Child Health and Development (NICHD) (NIH R01HD078561, R21HD069001) (E.T.) and the Ruth L. Kirschstein National Research Service Awards for Individual Postdoctoral Fellows (NIH F32 AR058105) (J.W.S.). This research was carried out in part at the Athinoula A. Martinos Center for Biomedical Imaging at the Massachusetts General Hospital, using resources provided by the Center for Functional Neuroimaging Technologies, NIH P41RR14075, a P41 Regional Resource supported by the Biomedical Technology Program of the National Center for Research Resources (NCRR), National Institutes of Health. This work also involved the use of instrumentation supported by the NCRR Shared Instrumentation Grant Program (NIH S10RR023401, S10RR019307, and S10RR 023043) and High-End Instrumentation Grant Program (NIH S10RR016811). This study was conducted partly using postmortem human brain specimens from the tissue collection at the Department of Neurobiology at Yale University School of Medicine (supported by grant NIH MH081896), which form a part of the BrainSpan Consortium collection (http://www.brainspan.org). The other brain specimens were provided by Dr Rebecca D. Folkerth, Brigham and Women's Hospital, Boston Children's Hospital, and Harvard Medical School.

Notes

Conflict of Interest: None declared.

References

Berman JI, Lanza MR, Blaskey L, Edgar JC, Roberts TP. 2013. High angular resolution diffusion imaging probabilistic tractography of the auditory radiation. AJNR Am J Neuroradiol. 34(8):1573–1578.

Buchel C, Raedler T, Sommer M, Sach M, Weiller C, Koch MA. 2004. White matter asymmetry in the human brain: a diffusion tensor MRI study. Cereb Cortex. 14:945–951.

Catani M, Thiebaut de Schotten M. 2008. A diffusion tensor imaging tractography atlas for virtual in vivo dissections. Cortex. 44(8): 1105–1132.

Caviness VS Jr, Kennedy DN, Richelme C, Rademacher J, Filipek PA. 1996. The human brain age 7–11 years: a volumetric analysis based on magnetic resonance images. Cereb Cortex. 6:726–736.

Chechlacz M, Rotshtein P, Hansen PC, Riddoch JM, Deb S, Humphreys GW. 2012. The neural underpinings of simultanagnosia: disconnecting the visuospatial attention network. J Cogn Neurosci. 24:718–735.

Chi JG, Dooling EC, Gilles FH. 1977. Left-right asymmetries of the temporal speech areas of the human fetus. Arch Neurol. 34:346–348.
D'Arceuil H, Liu C, Levitt P, Thompson B, Kosofsky B, de Crespigny A. 2008. Three-dimensional high-resolution diffusion tensor imaging and tractography of the developing rabbit brain. Dev Neurosci. 30:262–275.
Dehaene S, Pegado F, Braga LW, Ventura P, Nunes Filho G, Jobert A, Dehaene-Lambertz G, Kolinsky R, Morais J, Cohen L. 2010. How learning to read changes the cortical networks for vision and language. Science. 330:1359–1364.
Dehaene-Lambertz G, Hertz-Pannier L, Dubois J. 2006. Nature and nurture in language acquisition: anatomical and functional brain-imaging studies in infants. Trends Neurosci. 29:367–373.
Escalante-Mead PR, Minshew NJ, Sweeney JA. 2003. Abnormal brain lateralization in high-functioning autism. J Autism Dev Disord. 33:539–543.
Fontes V. 1944. Estudos de anatomia macroscópica do sistema nervoso central nas crianças posrtuguesas. Lisbon (Portugal): Instituto de Antonio Aurelio da Costa Ferreira.
Galaburda AM. 1993. Neuroanatomic basis of developmental dyslexia. Neurol Clin. 11:161–173.
Galaburda AM, Sherman GF, Rosen GD, Aboitiz F, Geschwind N. 1985. Developmental dyslexia: four consecutive patients with cortical anomalies. Ann Neurol. 18:222–233.
Gilmore JH, Lin W, Prastawa MW, Looney CB, Vetsa YS, Knickmeyer RC, Evans DD, Smith JK, Hamer RM, Lieberman JA et al. 2007. Regional gray matter growth, sexual dimorphism, and cerebral asymmetry in the neonatal brain. J Neurosci. 27:1255–1260.
Gogtay N, Giedd JN, Lusk L, Hayashi KM, Greenstein D, Vaituzis AC, Nugent TF 3rd, Herman DH, Clasen LS, Toga AW et al. 2004. Dynamic mapping of human cortical development during childhood through early adulthood. Proc Natl Acad Sci USA. 101: 8174–8179.
Gong G, Jiang T, Zhu C, Zang Y, Wang F, Xie S, Xiao J, Guo X. 2005. Asymmetry analysis of cingulum based on scale-invariant parameterization by diffusion tensor imaging. Hum Brain Mapp. 24: 92–98.
Halpern ME, Gunturkun O, Hopkins WD, Rogers LJ. 2005. Lateralization of the vertebrate brain: taking the side of model systems. J Neurosci. 25:10351–10357.
Heilbroner PL, Holloway RL. 1988. Anatomical brain asymmetries in new world and old world monkeys: stages of temporal lobe development in primate evolution. Am J Phys Anthropol. 76:39–48.
Herbert MR, Ziegler DA, Deutsch CK, O'Brien LM, Kennedy DN, Filipek PA, Bakardjiev AI, Hodgson J, Takeoka M, Makris N et al. 2005. Brain asymmetries in autism and developmental language disorder: a nested whole-brain analysis. Brain. 128:213–226.
Hill J, Dierker D, Neil J, Inder T, Knutsen A, Harwell J, Coalson T, van Essen D. 2010. A surface-based analysis of hemispheric asymmetries and folding of cerebral cortex in term-born human infants. J Neurosci. 30:2268–2276.
Hochestetter F. 1929. Beitrage zur Entwicklungsgeschichte des Menschlichen Gehirns. Leipzig Wien: Deuticke.
Huang H, Xue R, Zhang J, Ren T, Richards LJ, Yarowsky P, Miller MI, Mori S. 2009. Anatomical characterization of human fetal brain development with diffusion tensor magnetic resonance imaging. J Neurosci. 29:4263–4273.
Huttenlocher PR. 1979. Synaptic density in human frontal cortex - developmental changes and effects of aging. Brain Res. 163:195–205.
Huttenlocher PR, Dabholkar AS. 1997. Regional differences in synaptogenesis in human cerebral cortex. J Comp Neurol. 387: 167–178.
Innocenti GM, Clarke S, Kraftsik R. 1986. Interchange of callosal and association projections in the developing visual cortex. J Neurosci. 6:1384–1409.
Jenner AR, Rosen GD, Galaburda AM. 1999. Neuronal asymmetries in primary visual cortex of dyslexic and nondyslexic brains. Ann Neurol. 46:189–196.
Kasprian G, Langs G, Brugger PC, Bittner M, Weber M, Arantes M, Prayer D. 2011. The prenatal origin of hemispheric asymmetry: an in utero neuroimaging study. Cereb Cortex. 21:1076–1083.
Knickmeyer RC, Gouttard S, Kang C, Evans D, Wilber K, Smith JK, Hamer RM, Lin W, Gerig G, Gilmore JH. 2008. A Structural MRI Study of Human Brain Development from Birth to 2 Years. J Neurosci. 28(47):12176–12182.
Kolasinski J, Takahashi E, Stevens AA, Benner T, Fischl B, Zöllei L, Grant PE. 2013. Radial and tangential neuronal migration pathways in the human fetal brain: anatomically distinct patterns of diffusion MRI coherence. Neuroimage. 1(79):412–422.
Kostovic I, Vasung L. 2009. Insights from in vitro fetal magnetic resonance imaging of cerebral development. Semin Perinatol. 33:220–233.
Kucyi A, Moayedi M, Weissman-Fogel I, Hodaie M, Davis KD. 2012. Hemispheric asymmetry in white matter connectivity of the temporoparietal junction with the insula and prefrontal cortex. PLoS One. 7:e35589.
LaMantia AS, Rakic P. 1990. Axon overproduction and elimination in the corpus callosum of the developing rhesus monkey. J Neurosci. 10:2156–2175.
Lebel C, Beaulieu C. 2009. Lateralization of the arcuate fasciculus from childhood to adulthood and its relation to cognitive abilities in children. Hum Brain Mapp. 30:3563–3573.
Lebel C, Walker L, Leemans A, Phillips L, Beaulieu C. 2008. Microstructural maturation of the human brain from childhood to adulthood. Neuroimage. 40:1044–1055.
Mori S, Crain BJ, Chacko VP, van Zijl PC. 1999. Three-dimensional tracking of axonal projections in the brain by magnetic resonance imaging. Ann Neurol. 45:265–269.
Oertel-Knochel V, Linden DE. 2011. Cerebral asymmetry in schizophrenia. Neuroscientist. 17:456–467.
Ortibus E, Verhoeven J, Sunaert S, Casteels I, de Cock P, Lagae L. 2012. Integrity of the inferior longitudinal fasciculus and impaired object recognition in children: a diffusion tensor imaging study. Dev Med Child Neurol. 54:38–43.
Philippi CL, Mehta S, Grabowski T, Adolphs R, Rudrauf D. 2009. Damage to association fiber tracts impairs recognition of the facial expression of emotion. J Neurosci. 29:15089–15099.
Provenzale JM, Liang L, DeLong D, White LE. 2007. Diffusion tensor imaging assessment of brain white matter maturation during the first postnatal year. AJR Am J Roentgenol. 189:476–486.
Rajagopalan V, Scott J, Habas PA, Kim K, Corbett-Detig J, Rousseau F, Barkovich AJ, Blenn OA, Studholme C. 2011. Local tissue growth patterns underlying normal fetal human brain gyrification quantified in utero. J Neurosci. 31:2878–2887.
Rakic P, Yakovlev PI. 1968. Development of the corpus callosum and cavum septi in man. J Comp Neurol. 132(1):45–72.
Ribolsi M, Koch G, Magni V, Di Lorenzo G, Rubino IA, Siracusano A, Centonze D. 2009. Abnormal brain lateralization and connectivity in schizophrenia. Rev Neurosci. 20:61–70.
Schmahmann JD, Pandya DN. 2009. Fiber pathways of the brain. USA: Oxford Univ Press.
Schmahmann JD, Pandya DN, Wang R, Dai G, D'Arceuil HE, de Crespigny AJ, Wedeen VJ. 2007. Association fibre pathways of the brain: parallel observations from diffusion spectrum imaging and autoradiography. Brain. 130:630–653.
Simms MD, Schum RL. 2011. Language development and communication disorders. In: Kliegman RM, Stanton B, St Geme J, Schor NF, Behrman RE, editors. Nelson textbook of pediatrics. Philadelphia: W. B. Saunders. p. 114–121.
Song JW, Misgeld T, Kang H, Knecht S, Lu J, Cao Y, Cotman SL, Bishop DL, Lichtman JW. 2008. Lysosomal activity associated with developmental axon pruning. J Neurosci. 28:8993–9001.
Takahashi E, Dai G, Rosen GD, Wang R, Ohki K, Folkerth RD, Galaburda AM, Wedeen VJ, Ellen Grant P. 2011. Developing neocortex organization and connectivity in cats revealed by direct correlation of diffusion tractography and histology. Cereb Cortex. 21:200–211.
Takahashi E, Dai G, Wang R, Ohki K, Rosen GD, Galaburda AM, Grant PE, Wedeen VJ. 2010. Development of cerebral fiber pathways in cats revealed by diffusion spectrum imaging. Neuroimage. 49:1231–1240.
Takahashi E, Folkerth RD, Galaburda AM, Grant PE. 2012. Emerging cerebral connectivity in the human fetal brain: an MR tractography study. Cereb Cortex. 22:455–464.

Takahashi E, Ohki K, Kim DS. 2007. Diffusion tensor studies dissociated two fronto-temporal pathways in the human memory system. Neuroimage. 34:827–838.
Takahashi E, Ohki K, Kim DS. 2013. Dissociation and convergence of the dorsal and ventral visual streams in the human prefrontal cortex. Neuroimage. 65:488–498.
Takao H, Hayashi N, Ohtomo K. 2011. White matter asymmetry in healthy individuals: a diffusion tensor imaging study using tract-based spatial statistics. Neuroscience. 193:291–299.
Thiebaut de Schotten M, Ffytche DH, Bizzi A, Dell'Acqua F, Allin M, Walshe M, Murray R, Williams SC, Murphy DG, Catani M. 2011. Atlasing location, asymmetry and inter-subject variability of white matter tracts in the human brain with MR diffusion tractography. Neuroimage. 54:49–59.
Tuch DS, Reese TG, Wiegell MR, Wedeen VJ. 2003. Diffusion MRI of complex neural architecture. Neuron. 40:885–895.
Vasung L, Jovanov-Milosevic N, Pletikos M, Mori S, Judas M, Kostovic I. 2011. Prominent periventricular fiber system related to ganglionic eminence and striatum in the human fetal cerebrum. Brain Struct Funct. 215:237–253.
Vishwas MS, Chitnis T, Pienaar R, Healy BC, Grant PE. 2010. Tract-based analysis of callosal, projection, and association pathways in pediatric patients with multiple sclerosis: a preliminary study. AJNR Am J Neuroradiol. 31:121–128.
Wedeen VJ, Wang RP, Schmahmann JD, Benner T, Tseng WY, Dai G, Pandya DN, Hagmann P, D'Arceuil H, de Crespigny AJ. 2008. Diffusion spectrum magnetic resonance imaging (DSI) tractography of crossing fibers. Neuroimage. 41:1267–1277.
Xu G, Takahashi E, Folkerth RD, Haynes RL, Volpe JJ, Grant PE, Kinney HC. 2014. Radial coherence of diffusion tractography in the cerebral white matter of the human fetus: neuroanatomic insights. Cereb Cortex. 24:579–592.
Yin X, Han Y, Ge H, Xu W, Huang R, Zhang D, Xu J, Fan L, Pang Z, Liu S. 2013. Inferior frontal white matter asymmetry correlates with executive control of attention. Hum Brain Mapp. 34: 796–813.